

Oxidative Esterification of Aldehydes Using Mesoionic 1,2,3-Triazolyl Carbene Organocatalysts

Matthew T. Berry, Disnay Castrejon, and Jason E. Hein*

Department of Chemistry and Chemical Biology, University of California, 5200 North Lake Road, Merced, California 95343, United States

Supporting Information

ABSTRACT: The synthesis and catalytic activity of a new class of 1,2,3-triazolyl *N*-heterocyclic carbene organocatalysts is described. These new catalysts chemoselectively facilitate the oxidative esterification of aldehydes. NMR acidity studies show an inverse correlation between triazolium acidity and reactivity. Kinetic studies show that the resting state of the catalyst involves a NHC–aldehyde adduct. A catalytically active intermediate was synthesized and characterized by X-ray diffraction as the initial carbene–aldehyde adduct.

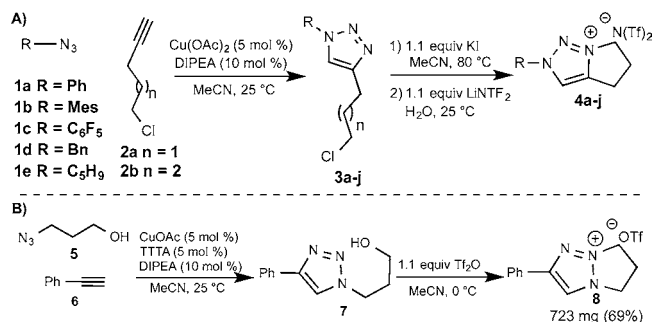


The development of *N*-heterocyclic carbene catalysis in the past 50 years has led to the discovery of a wide library of synthetic transformations.¹ Recent work in this field by Enders,^{2,3} Bode,^{4,5} Rovis,^{6,7} and Scheidt^{8,9} has led to the development of new carbene catalysts that feature the thiazolyl, imidazolyl, and 1,2,4-triazolyl architectures. Despite the wide structural diversity explored within these systems, the feature common to all is the singlet carbene center flanked by two heteroatomic neighbors, resulting in a stabilized neutral carbene. Recently, Bertrand reported the synthesis, isolation, and characterization of a new class of mesoionic carbene based on the 1,2,3-triazolium scaffold.^{10,11} These unique carbenes, sometimes termed remote or abnormal *N*-heterocyclic carbenes, bear only a single flanking heteroatom and exist as a zwitterionic structure with no neutral canonical resonance form. Because these carbenes possess a unique electronic structure, they are desirable as potential nucleophilic organocatalysts.

In addition to these unique electronic properties, the 1,2,3-triazolium core represents a highly modifiable catalyst architecture, making the 1,2,3-triazolyl carbene an attractive catalyst candidate. Via a simple two-step synthetic sequence (Scheme 1), a variety of precatalysts with differing electronic and steric properties were obtained quickly and cleanly. Two possible regioisomers are accessible through this synthetic strategy: the 1,3,4-substituted and 1,2,4-substituted 1,2,3-triazolium salts. By varying the substituents of the azide and alkyne precursors, both of these regioisomers can be obtained. Herein we report the first demonstration of these compounds as organocatalysts that facilitate the oxidative esterification of aldehydes.

The candidate triazolium salts were synthesized via a simple two-step protocol (Scheme 1). To obtain the 1,3,4-substituted triazolium salts **4a–j**, azides **1a–e** were coupled to alkyne **2a** or **2b** via the Cu-catalyzed azide–alkyne cycloaddition.¹² The resulting triazoles **3a–j** were then cyclized and underwent ion

Scheme 1. Synthesis of Triazolium Salt Precatalysts



exchange with LiNTf₂ to give triazolium salts **4a–j**.¹³ Similarly, the 1,2,4-trisubstituted-1,2,3-triazolium salt **8** was formed via coupling azide **5** with alkyne **6**, followed by cyclization of triazole **7** with (Tf)₂O to yield **8**. These protocols allowed for a diverse set of triazolium salts to be rapidly prepared on multigram scale (Figure 1).

To test the catalytic activity of the triazolium salts, we screened different common NHC-catalyzed reactions (benzoin condensation, Stetter reaction,¹⁴ and redox esterification¹⁵) with **4c** as a trial catalyst. While these trials did not yield any of the expected products, we did find that our catalyst facilitated the oxidative esterification of cinnamaldehyde with methanol in trace yields. By introducing quinone **12** as oxidant instead of ambient molecular oxygen, our yields improved (Scheme 2). To optimize reaction conditions and gain mechanistic insight, we used reaction monitoring techniques (HPLC, NMR, React-IR) to understand the individual contributions of each reaction component and to identify the cause of catalyst deactivation.

Received: May 20, 2014

Published: July 2, 2014

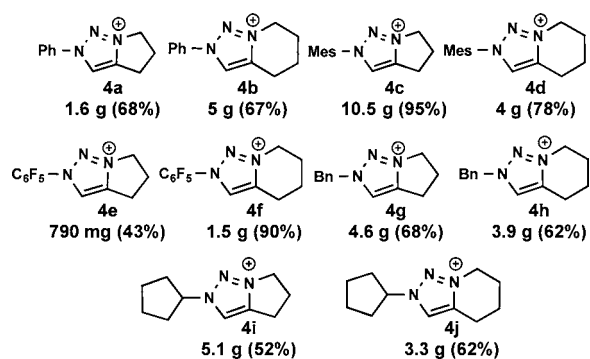
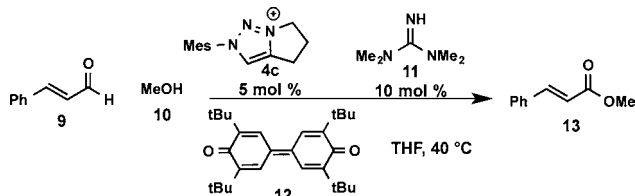


Figure 1. Scope of 1,2,3-triazolium salt precatalysts. Counterion for all salts is bis(trifluoromethane)sulfonamide (NTf_2^-).

Scheme 2. Initial Trial Reaction Conditions



Initially, we considered the possibility that the overall moderate catalytic performance of these species was due to a low population of the free carbene catalyst, stemming from a lack of acidity at the C5 proton. To probe this possibility, we used in situ NMR to monitor the rate of deuterium incorporation at the C5 position starting from the protonated azolium precatalyst in the presence of DIPEA (Figure 2a). This experiment demonstrates that both the *N*-substituent and exocyclic ring size impact the relative acidity of the azolium C–H. Precatalysts with strongly electron-poor aromatic substituents (4e and 4f) showed the fastest rate of exchange, whereas species with the more electron-rich mesityl substitution (4c and 4d) display the slowest exchange. While it appears that the *N*-substituent plays the largest role in modifying the triazolium acidity, the size of the saturated ring also has an impact. In general, triazoliums bearing a five-membered ring display faster rates of deuterium incorporation than their corresponding six-membered analogues (Figure 2a, 4a cf. 4b; 4c cf. 4d).

Following this survey, we attempted to correlate the precatalyst's relative acidity (as implied from the observed deuterium incorporation rates) with their catalytic efficiency. Individually, triazoliums 4a–f were applied to the oxidative esterification of cinnamaldehyde, and product formation was monitored by HPLC (Figure 2b). This experiment revealed two key trends. First, the size of the saturated ring plays a larger role in catalytic efficiency than the nature of the *N*-aryl substituent, with the most effective catalysts 4a and 4c both containing the 5-membered subunit. This result may be due to unfavorable steric encumbrance adjacent to the carbene center leading to hindered nucleophilicity. Second, the catalytic activity appears to be inversely proportional to the relative acidity of the triazolium species. Electron-poor C_6F_5 -substituted triazoliums (4e and 4f) performed very poorly, while mesityl-substituted 4c displayed the highest efficiency.

Moreover, electron-poor 4e and 4f display no further conversion beyond 5 h, leading us to conclude that rapid deactivation is the root cause of the poor performance of

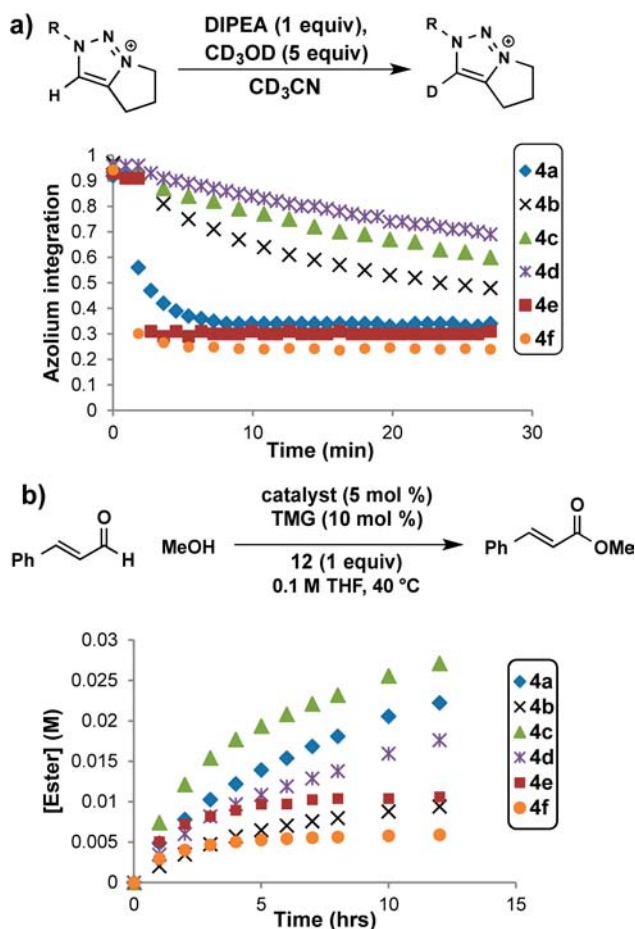
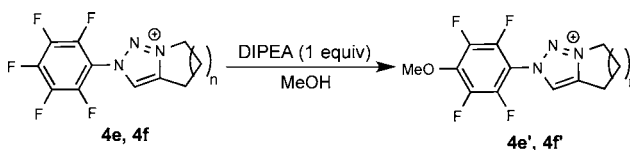


Figure 2. (a) Deuterium exchange curves for each 1,2,3-triazolium salt. (b) Reaction progress curves for each 1,2,3-triazolium salt.

these species. In part, this hypothesis is supported by the detection of a decomposition product 4e' by HPLC–MS, believed to result from a $\text{S}_{\text{N}}\text{Ar}$ -type addition of methanol to the C_6F_5 ring (Scheme 3). While we were unable to isolate

Scheme 3. Possible Decomposition Pathway of C_6F_5 -Substituted Triazolium Catalysts



4e' for full characterization, we have confirmed that 4e and 4f are both stable in solutions of MeOH but rapidly form 4e' and 4f' on addition of base. This result suggests that the pendant azolium group is an effective electrophilic activator of the perfluoroaromatic group.

Ruling out carbene population as the reason for low yields, we turned to investigating the individual contribution of each component to the rate of product formation. Multiple reactions with differing initial concentrations of either cinnamaldehyde, TMG, MeOH, or oxidant 12 were performed and monitored by HPLC sampling, giving reaction progress curves (see the Supporting Information). Plotting the initial rate of the oxidative esterification as a function of the initial concentration for each component being varied (Figure

3) allows us to identify which reagents are involved in the rate-limiting step and suggest a resting state for the catalyst.

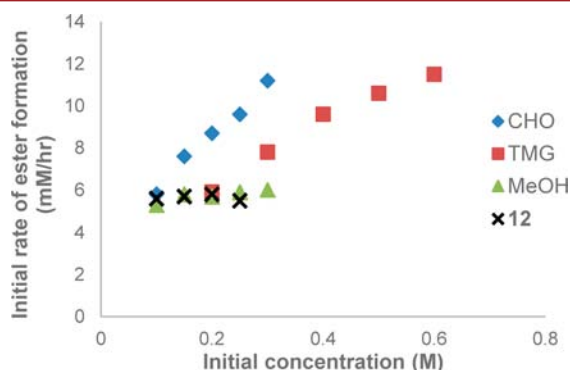
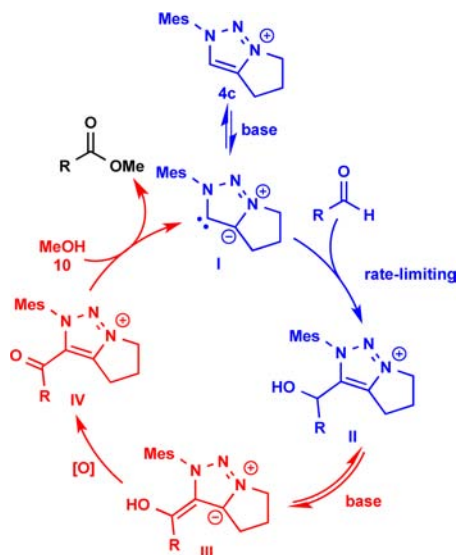


Figure 3. Plot of initial rate vs initial concentration for each reaction component. The zero slope of the MeOH and 12 curves indicate the reaction is zero-order in both components. The positive slope in the aldehyde and TMG curves shows the reaction to be positive order in those components.

Our study revealed that changes in the initial concentration of both MeOH and oxidant 12 do not impact the observed rate, and thus, the reaction is zero-order with respect to these reagents (Figure 3). By contrast, increasing concentrations of both cinnamaldehyde and TMG lead to an increase in reaction rate; however, the rate enhancement due to additional TMG does reach a saturation point beyond 0.8 M. These results can be explained in the context of the catalytic cycle (Scheme 4). Since both MeOH and 12 do not

Scheme 4. Proposed Catalytic Cycle

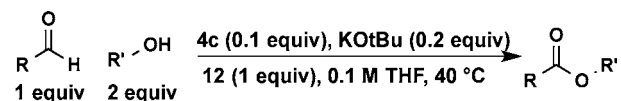


affect initial reaction rate, we can conclude that both the oxidation and nucleophilic substitution are not rate limiting (Scheme 4, III \rightarrow IV and IV \rightarrow I, respectively). However, both TMG and cinnamaldehyde must be involved in kinetically important steps, suggesting that the resting state of the catalyst is not clearly defined as a single intermediate. Instead, it is possible that the rate constants for the formation of the free carbene I, addition of aldehyde to generate II and

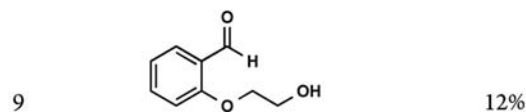
isomerization to Breslow-like intermediate III all have similar magnitude under these reaction conditions.

In addition to informing us of the possible mechanism, our studies provided us with optimized conditions to carry out the esterification. Running the reaction with 2 equiv of alcohol and increasing catalyst loading to 10 mol % improved yields and reaction times. Screening a variety of organic and inorganic bases revealed that 0.2 equiv of KOTBu was optimal, allowing reaction time to be reduced from 48 to 3 h. A brief substrate scope of this reaction was performed using these newly optimized conditions (Table 1). Electron-withdrawing

Table 1. Substrate Scope^a



entry	R	R'	yield ^b
1	PhCH=CH	Me	82%
2	PhCH=CH	iPr	12%
3	PhCH=CH	Bn	63%
4	4-Cl-C ₆ H ₅	Me	11%
5	4-NO ₂ -C ₆ H ₅	Me	86%
6	4-OMe-C ₆ H ₅	Me	N/A
7	2-pyridyl	Me	74%
8	2-naphthyl	Me	57%



^aStandard reaction conditions: aldehyde (0.5 mmol, 1 equiv), alcohol (1 mmol, 2 equiv), 12 (0.5 mmol, 1 equiv), and 4c (0.05 mmol, 0.1 equiv) were dissolved in anhydrous THF and heated to 40 °C. KOTBu (0.1 mmol, 0.2 equiv) was added and the mixture heated overnight.
^bIsolated yield after column chromatography.

groups (entry 5) and heterocyclic substituents (entry 7) are tolerated, while electron-donating aryl substrates (entry 6) do not react. Primary alcohol nucleophiles are the most effective, while secondary alcohols are far less reactive. These catalysts also facilitate intramolecular cyclizations (entry 9), however, reactions with *t*-BuOH or phenols give little to no product.

During the course of our reaction progress investigations, we observed an intermediate by HPLC/MS with a mass that corresponds to a carbene-aldehyde adduct. This compound could be one of three tautomeric forms arising from the nucleophilic addition of free catalyst I with the aldehyde (Figure 4a, 14, 15, and 16).^{16,17}

In hopes of isolating this intermediate for further identification, we carried out a series of reactions where oxidant 12 was omitted. The catalyst, aldehyde, base, and solvent were varied and the intermediate formation and decomposition was monitored by HPLC/MS (see the Supporting Information for progress curves). Reacting triazolium 4c with 4-chlorobenzaldehyde and NaOH appeared to produce the desired intermediate in highest concentration (Figure 4a). Using these conditions, we successfully isolated and unambiguously characterized this compound by NMR

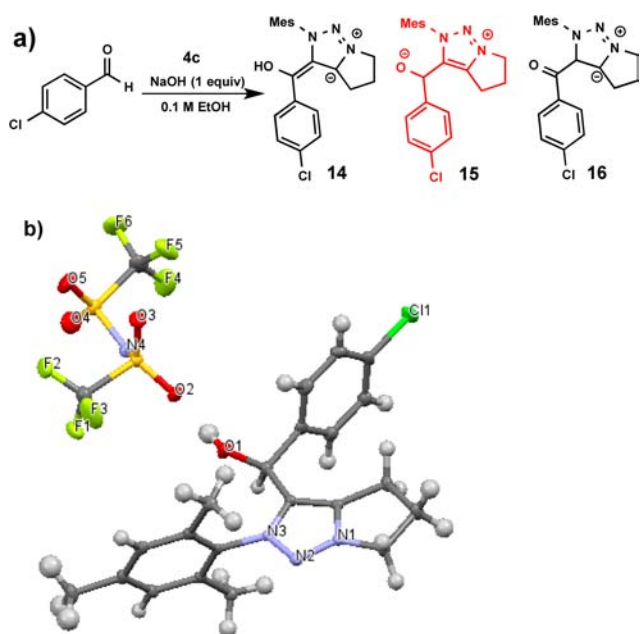
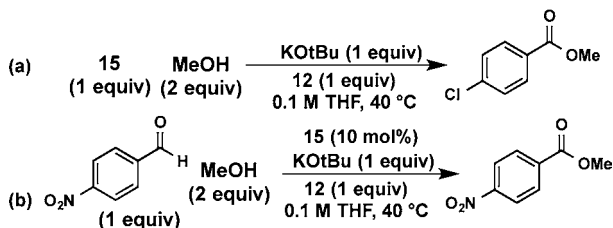


Figure 4. (a) Possible tautomers of the catalytic intermediate formed from 4-chlorobenzaldehyde and **4c**. (b) X-ray crystal structure of isolated catalytic intermediate **15**.

and single-crystal X-ray diffraction, revealing that it is in fact the benzylic alcohol carbene-aldehyde adduct **15**.

Isolation and identification of **15** allows us to further refine our mechanistic interpretation. This intermediate is stable in solid form but can be reverted to free carbene and aldehyde on treatment with base. Treating **15** solely with oxidant **12** or with DDQ to allow direct benzylic oxidation were all unsuccessful. However, subjecting **15** to the reaction conditions including KOtBu, MeOH, and **12** did result in ester formation (Scheme 5a). In addition, **15** can be used to convert 4-nitrobenzaldehyde to the corresponding ester, demonstrating its competence as a precatalyst for further reaction (Scheme 5b).

Scheme 5. Catalytic Activity of Isolated Intermediate **15**



Together these results confirm that the esterification likely proceeds first via nucleophilic capture of the aldehyde by the mesoionic carbene to give **II**, followed by proton transfer to give the Breslow-like intermediate **III** and subsequent oxidation, instead of a direct oxidation pathway from **II** to **IV**.

In conclusion, we have demonstrated the first report of organocatalytic activity for mesoionic 1,2,3-triazolyl carbenes. We have identified the likely resting state and have isolated a catalytic intermediate, proving that these carbenes act as nucleophilic organocatalysts.

■ ASSOCIATED CONTENT

Supporting Information

Experimental procedures, characterization data, reaction progress curves, and X-ray crystal data. This material is available free of charge via the Internet at <http://pubs.acs.org>.

■ AUTHOR INFORMATION

Corresponding Author

*E-mail: jhein2@ucmerced.edu.

Notes

The authors declare no competing financial interest.

■ ACKNOWLEDGMENTS

Funding from UCM (Graduate and Research Council Faculty Award). Further support was provided by NSF-COINS EEC-0832819. We thank Dr. Arnold Rheingold and Dr. Curtis Moore at the UCSD Crystallography Laboratory and Dr. Alfred D. Bacher at UCLA for generous use of FTIR.

■ REFERENCES

- (1) For reviews on NHC organocatalysis, see: (a) Enders, D.; Niemeier, O.; Henseler, A. *Chem. Rev.* **2007**, *107*, 5606–5655. (b) Grossmann, A.; Enders, D. *Angew. Chem., Int. Ed.* **2012**, *51*, 314–325. (c) Chauhan, P.; Enders, D. *Angew. Chem., Int. Ed.* **2014**, *53*, 1485–1487.
- (2) Enders, D.; Breuer, K.; Teles, J. H. *Helv. Chim. Acta* **1996**, *79*, 1217–1221.
- (3) Enders, D.; Kallfass, U. *Angew. Chem., Int. Ed.* **2002**, *41*, 1743–1745.
- (4) Sohn, S. S.; Bode, J. W. *Org. Lett.* **2005**, *7*, 3873–3876.
- (5) Sohn, S. S.; Bode, J. W. *Angew. Chem., Int. Ed.* **2006**, *45*, 6021–6024.
- (6) Reynolds, N. T.; Rovis, T. *J. Am. Chem. Soc.* **2005**, *127*, 16406–16407.
- (7) Kerr, M. S.; Alaniz, J. R. De; Rovis, T. *J. Org. Chem.* **2005**, *70*, 5725–5728.
- (8) Mattson, A. E.; Bharadwaj, A. R.; Zuhl, A. M.; Scheidt, K. A. *J. Org. Chem.* **2006**, *71*, 5715–5724.
- (9) Chan, A.; Scheidt, K. A. *J. Am. Chem. Soc.* **2006**, *128*, 4558–4559.
- (10) Guisado-Barrios, G.; Bouffard, J.; Donnadieu, B.; Bertrand, G. *Angew. Chem.* **2010**, *122*, 4869–4872.
- (11) Bouffard, J.; Keitz, B. K.; Tonner, R.; Lavallo, V.; Guisado-Barrios, G.; Frenking, G.; Grubbs, R. H.; Bertrand, G. *Organometallics* **2011**, *30*, 2617–2627.
- (12) Hein, J. E.; Fokin, V. V. *Chem. Soc. Rev.* **2010**, *39*, 1302–1315.
- (13) Tseng, M.; Cheng, H.; Shen, M.; Chu, Y. *Org. Lett.* **2011**, *13*, 4434–4437.
- (14) Stetter, H. *Angew. Chem., Int. Ed. Engl.* **1976**, *15*, 639–712.
- (15) Mahatthananchai, J.; Bode, J. W. *Chem. Sci.* **2012**, *3*, 192–197.
- (16) Alwarsh, S.; Ayinuola, K.; Dormi, S. S.; McIntosh, M. C. *Org. Lett.* **2013**, *15*, 3–5.
- (17) Berkessel, A.; Elfert, S.; Etzenbach-Effers, K.; Teles, J. H. *Angew. Chem., Int. Ed.* **2010**, *49*, 7120–7124.